Frontiers in Bioscience Scholar

Front. Biosci. (Schol Ed) **2025**; 17(1): 27967
https://doi.org/10.31083/FBS27967

Original Research

Aquaporins as Membrane Proteins: The Current Status

Irena Roterman[1,*], Katarzyna Stapor[2], Dawid Dułak[3], Grzegorz Szoniec[4], Leszek Konieczny[5]

[1]Department of Bioinformatics and Telemedicine, Jagiellonian University-Medical College, 30-688 Krakow, Medyczna 7, Poland
[2]Faculty of Automatic, Electronics and Computer Science, Department of Applied Informatics, Silesian University of Technology, Akademicka 16, 44-100 Gliwice, Poland
[3]ABB Business Services Sp. z o.o, ul Żegańska 1, 04-713 Warszawa, Poland
[4]Jagiellonian University Medical College, 30-008 Krakow, Poland
[5]Chair of Medical Biochemistry, Jagiellonian University - Medical College, 31-034 Krakow, Kopernika 7, Poland
*Correspondence: myroterm@cyf-kr.edu.pl (Irena Roterman)
Academic Editor: Ioanna-Katerina Aggeli
Submitted: 8 November 2024 Revised: 16 December 2024 Accepted: 6 February 2025 Published: 20 March 2025

Abstract

Background: The ambient conditions that ensure the expected protein folding activity are important in directing the protein folding process. Water favors the formation of a centrally located hydrophobic protein nucleus with exposed polar residues for preferable contact with polar water molecules. Different ambient conditions are created by the hydrophobic cell membrane, which also provides an environment for the activity of proteins, including channels responsible for transporting multiple molecules, the concentration of which is controlled as part of homeostasis. Aquaporins are transmembrane proteins responsible for primarily transporting water and low-molecular-weight compounds. **Methods**: The fuzzy oil drop (FOD) model was applied in its modified form, FOD-M, for the analysis. The FOD model allows quantitative assessment of protein structure adaptation to external conditions, ensuring its biological activity. **Results**: The aquaporins studied in this work revealed adaptations for stabilizing hydrophobic environments and transporting polar molecules. **Conclusions**: A significant degree of similarity was demonstrated in the structure of human aquaporins using FOD-M. This model enabled a quantitative assessment of the degree of adaptation to biological function achieved through an appropriate balance between micelle-like decomposition and appropriate modification due to the specificity of the environment that ensures adequate activity.

Keywords: aquaporins; water transport; protein membrane

1. Introduction

Water is the basic and natural environment for life; it is described as the "solvent of life" [1]. However, water content within a particular organelle (also a cell) of an organism must be controlled to ensure appropriate activity; thus, aquaporins regulate water content as a component of system-wide homeostasis [2]. Meanwhile, water transportation is also possible due to osmotic, diffusive effects [3–6]. However, this represents a marginal contribution to the transport of water molecules. Aquaporins ensure fast transportation through the phospholipid bilayer compared to osmotic diffusion. Furthermore, aquaporin transport is highly selective and limited solely to water molecules, with ions and other solutes excluded, meaning aquaporins selectively conduct water molecules in and out of the cell. However, since ions and other solutes are excluded, selectivity is required. The specific localization of Ans on the surface of the channel caused the water transport to associate this action with "roll a ball" [7,8]. Aquaporin 3 (AQP3) is involved in the wider spectrum of transported molecules, including water, glycerol, and hydrogen peroxide [9]. Meanwhile, AQP1 and AQP4 are aquaporins that operate in the nervous system [10].

Cotransporters and uniporters, proteins that are different from aquaporins, are also involved in the controlled transport of water across the cell membrane [11,12].

Special interest is being focused on the therapeutic aspects of aquaporins, especially in the brain or spinal cord [13], the early and acute phase of stroke [14], and the immune system [15,16]. Astrocyte swelling in hypothermia appears strongly related to AQP4 [17].

The aquaporin 4 isoform has also been recognized as a component in regulating brain cell assemblies in healthy individuals and autoimmune brain diseases that target aquaporin 4 [18,19]. Computer-aided drug design is focused on validated aquaporins as potential targets in neurodegenerative diseases [20].

Aquaporins represent a good example for analyzing the status of active membrane proteins in the hydrophobic cell membrane. Numerous examples of membrane-anchored proteins have been discussed and characterized based on analyses of the hydrophobicity distribution in the protein body [21–26]. Here, the structural specificity of the membrane protein responsible for water transport is discussed in the context of potential numerical techniques to simulate the protein folding process, which is different for membrane proteins than proteins active in aqueous environ-

Table 1. A list of the recognized proteins in the PDB database using the keyword "aquaporin".

PDB ID	Type	Chains	Chain length (amino acids)	Ref
1H6I	1	A	225	[28]
4NEF	2	A, B, C, D	239	[29]
6QF5	2	A	228	[30]
3DG8	4	A	223	[31]
3D9S	5	A, B, C, D	245	[32]
5C5X	5	A, B, C, D E, F, G, H	244	[33]
6QZI	7	A	247	[34]
6QZJ	7	A	245	[34]
4CSK		A	233	[35]

A brief structural characterization is also provided. The proteins were ordered by aquaporin class.

ments. The structure of aquaporins is described based on a modified version of the fuzzy oil drop (FOD) model with an expanded component that considers the hydrophobic membrane environment (FOD-M) [21–26].

The analysis presented in this paper discusses the protein structure dependence on the external force field during the folding process, leading to construction, which ensures activity in different surroundings, specifically in the hydrophobic membrane. The analysis includes the large spectrum of other proteins, including those folded and acting in a water environment. However, the proteins that require and collaborate with chaperones until they reach their structure, in the isolation conditions, form water solvents—in chaperonins. A comparison of these different protein groups forms the dogma regarding determining the 3D structure solely using the amino acid sequence, which requires additional aspects. The amino acid sequence with active participation in the external force field determines the 3D structure; for example, amyloids that represent diametrically different structures (native and amyloid) without any mutation. The FOD-M model, which can quantitatively assess the influence of the external force field on protein structure, was applied to a group of membrane proteins to determine the specificity of the aquaporin structure related to their environment and activity.

2. Materials and Methods

2.1 Data

Ten human proteins were identified in the Protein Data Bank (PDB) database https://www.rcsb.org/ [27] using the keyword "aquaporin" (Table 1, Ref. [28–35]).

2.2 Description of the FOD-M Model Used

This model has been extensively described previously [36]. The summary description below is intended to facilitate the interpretation of the presented results.

The FOD model assumes protein folding in the environment follows a micellization mechanism. Amino acids are treated as bi-polar molecules with varying polarity/hydrophobicity relationships. Such molecules in a polar water environment tend to isolate the hydrophobic parts in the center of the molecule with exposure of the polar residues for favorable contact with the polar water environment. Such an arrangement can be described by a three-dimensional (3D) Gaussian function spanning the body of the protein.

$$H_i^T = \frac{1}{H_{sum}^T} \exp\left(\frac{-(x_i-\bar{x})^2}{2\sigma_x^2}\right) \exp\left(\frac{-(y_i-\bar{y})^2}{2\sigma_y^2}\right) \exp\left(\frac{-(z_i-\bar{z})^2}{2\sigma_z^2}\right) \quad (1)$$

The values of the σ_x, σ_y, and σ_z parameters, adjusted to the shape and size of the molecule, facilitate the determination of the level of hydrophobicity in the position of the effective atom (the averaged position of the atoms comprising a given amino acid). Such a value represents an idealized, theoretical level assuming a micelle-like system—referred to here as "T".

Note that this distribution is determined for a specific orientation of the molecule in space: The geometric center is localized in the (0,0,0) point in the coordinate system, and the longest line connecting the two effective atoms determines the position of the x-axis. The longest line connecting the projection points on the YZ plane determines the orientation of the y-axis. The distances 0-x_{max}, 0-y_{max}, and 0-z_{max} determine the values of σ_x, σ_y, and σ_z, respectively, according to the three-sigma rule.

The actual level of hydrophobicity represented by a given effective atom is the effect of the inter-residual interaction expressed by the function proposed by Levitt M [37].

$$H_i^o = \frac{1}{H_{sum}^o} \sum_j \begin{cases} (H_i^r + H_j^r)\left(1 - \frac{1}{2}\left(7\left(\frac{r_{ij}}{c}\right)^2 - 9\left(\frac{r_{ij}}{c}\right)^4 + 5\left(\frac{r_{ij}}{c}\right)^6 - \left(\frac{r_{ij}}{c}\right)^8\right)\right) & \text{for } r_{ij} \le c \\ 0, \quad \text{for } r_{ij} > c \end{cases} \quad (2)$$

the c-cutoff distance (following [37] 9 Å was taken in calculations). The H^r expresses the intrinsic hydrophobicity of each amino acid (any hydrophobicity scale can be applied). The magnitude of this interaction depends on the distance between the interacting effective atoms and their intrinsic hydrophobicity. This distribution is referred to here as "O".

Normalization of the two distributions (the first expressions in the formulae) allows the two distributions to be compared quantitatively using the divergence entropy proposed by Kullback-Leibler [38].

$$D_{KL}(P \mid Q) = \sum_{i=1}^{N} P_i \log_2 \frac{P_i}{Q_i} \quad (3)$$

where P is the distribution under analysis (in our model, distribution O) and Q is the reference distribution (in our model, distribution T).

The D_{KL} value as an entropy-determining value cannot be interpreted quantitatively without comparing it to a reference distribution, which is a distribution with no differentiation in hydrophobicity levels (a distribution without a hydrophobic core). Such a distribution is expressed by the values $R_i = 1/N$, where N is the number of amino acids in the chain.

The relative distance (RD) parameter was introduced to assess the level of similarity of distribution O for the two distributions, T and R.

$$RD = \frac{D_{KL}(O \mid T)}{D_{KL}(O \mid T) + D_{KL}(O \mid R)} \tag{4}$$

an RD value <0.5 indicates the presence of a hydrophobic nucleus. An RD value >0.5 suggests a lack of conformity of distribution O vis-à-vis distribution T. This can vary because a local inconsistency attributed to specific residuals can raise the RD value, or the whole distribution is different than expected. In the first case, elimination of the residues with locally high incompatibility resulting in an RD <0.5 very often reveals the location of catalytic residues (hydrophobicity deficit) or a local hydrophobicity exposure (potential complexation site of another protein with similar hydrophobicity exposure).

In the second case, the entire distribution O differs from distribution T, which indicates a different folding mechanism that does not tend to generate a hydrophobic core. To explain this phenomenon, membrane proteins are a good example, where the expected distribution of hydrophobicity is opposite. For membrane proteins, an exposure of hydrophobicity with the localization of polar residues in the center of the protein molecule is expected (especially if the membrane protein acts as a channel for the transport of various chemicals). In this situation, the expected distribution is expressed by this function:

$$M_i = 1 - T_i \tag{5}$$

in practice, the following form is used:

$$M_i = T_{MAX} - T_i \tag{6}$$

with T_{MAX} being the maximum value in distribution T.

However, it turns out that the distribution of hydrophobicity in membrane proteins is a distribution that is the combination of distribution T and the distribution expressed by Eqn. 6. Thus, the final form representing the distribution in proteins can be described by the function M_i:

$$M_i = [T_i + K^* [T_{MAX} - T_i]_n]_n \tag{7}$$

with the parameter K denoting the degree to which the field disturbance from polar water was introduced with the orientation of the hydrophobicity distribution as a 3D Gaussian function. The M function with K = 0.0 represents the proteins with the micelle-like organization of hydrophobicity in the protein body.

The search for the form of the function M_i with an appropriately adjusted value of the parameter K allows the contribution of factors distinct from polar water (in the issue analyzed here, the contribution of hydrophobic molecules in particular), factors that shape the final form of the hydrophobicity distribution (the final form of the function M_i), to be determined.

The aquaporin proteins discussed in the present work can be characterized by assessing the type of hydrophobicity distribution through the value of the parameter RD—an assessment of the degree of ordering of hydrophobicity concerning the micelle-like arrangement—and the value of the parameter K, which determines the degree of external force participation changing the environment characteristics (presence of other than water molecules). In the case of aquaporins, the contribution of these different factors is interpreted as the contribution of the hydrophobic environment of the membrane.

A graphical representation of the FOD-M model used is shown in Fig. 1.

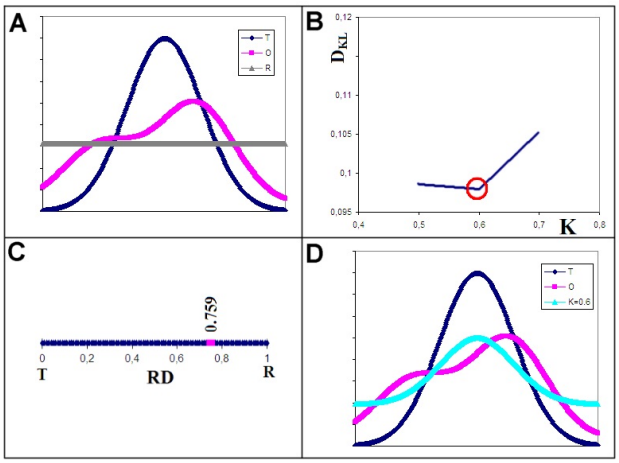

Fig. 1. Visualization of the fuzzy oil drop model (FOD-M) in its modified version—a one-dimensional version is provided for simpler presentation. (A) Summary of T, O, and R distributions. (B) The relative distance (RD) value determined for A suggests a lack of ordering consistent with a micelle-like arrangement. (C) Determination of the parameter K values—minimum value for D_{KL} for (O|M). (D) Summary of T, O, and M (green) distributions for K = 0.6.

The interpretation of the simplified example (Fig. 1) implies the absence of a hydrophobic nucleus (RD >0.5) and a significant contribution of non-aqueous factors in shaping the structure represented by the indicated T, O, and R distributions, expressed by K = 0.6.

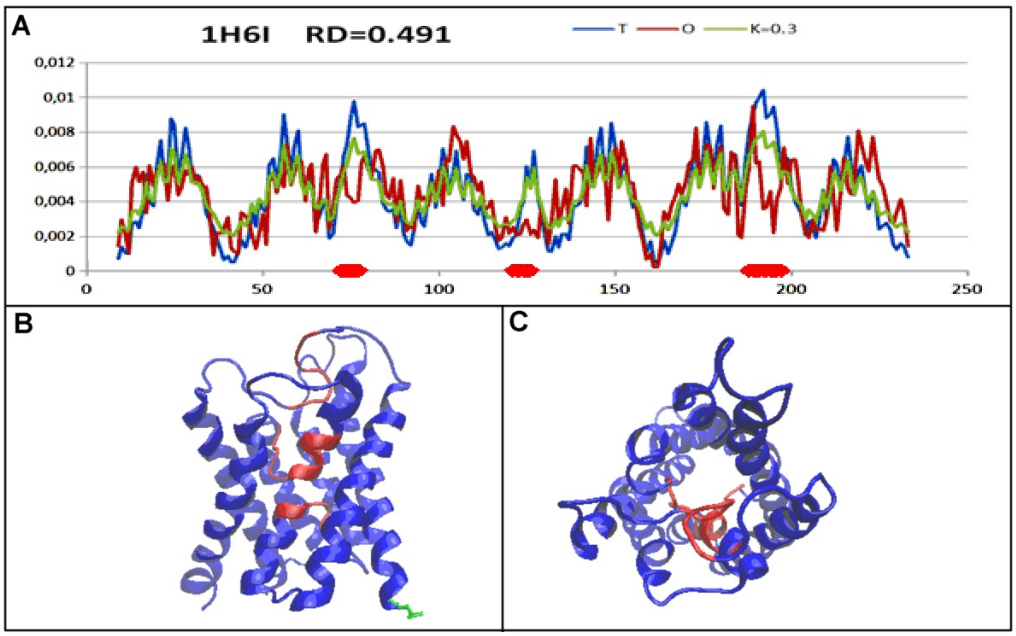

Fig. 2. Characteristics of 1H6I. (A) Summary of T, O, and M profiles for the corresponding K. Items highlighted in red on the horizontal axis are residuals showing a deficit in hydrophobicity. (B,C) Different 3D orientations of the structure with highlighted sections of local hydrophobicity deficit (in red). The residuals highlighted in green are the N-terminal position.

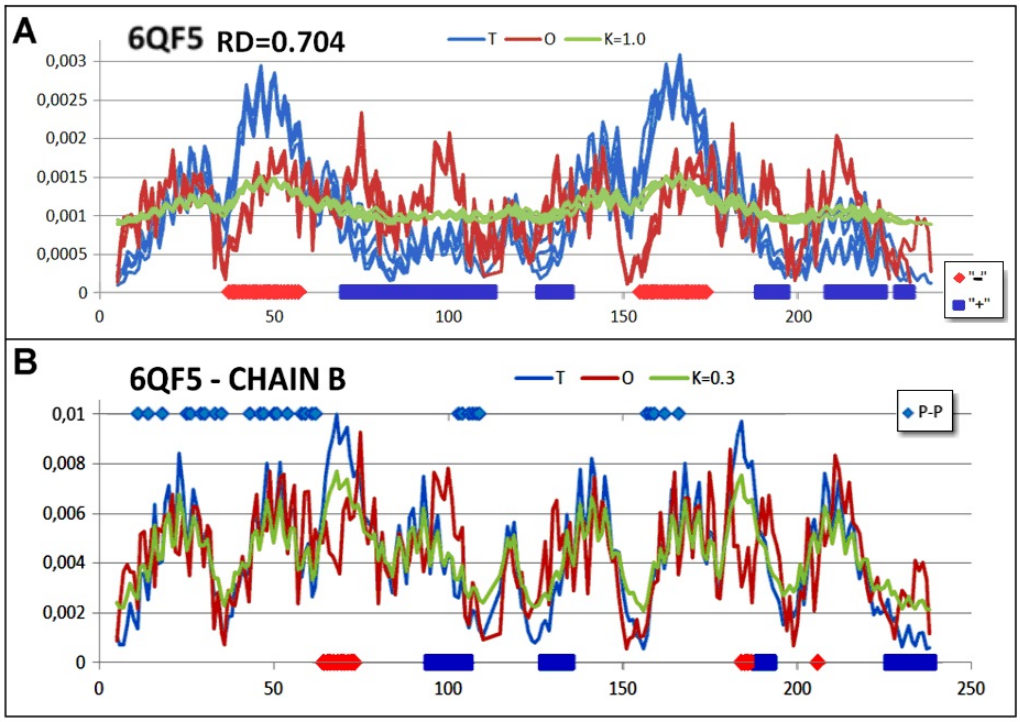

Fig. 3. Characteristics of 6QF5—aquaporin class 2. (A) Summary of T, O, and M profiles for the corresponding K value, characterizing the complex (four chains, superimposed). Red items: local hydrophobicity deficit ("-"); blue ("+") items: local hydrophobicity excess. (B) Summary of T, P, and M profiles for the respective K value, characterizing a single chain—parameters determined by treating the chain as an individual structural unit (3D Gaussian function spanning a single chain). The axis X represents the sequence that distinguishes between sections showing a deficit of hydrophobicity (red) and a local excess of hydrophobicity (blue). Residues involved in inter-chain interactions are highlighted on the top axis.

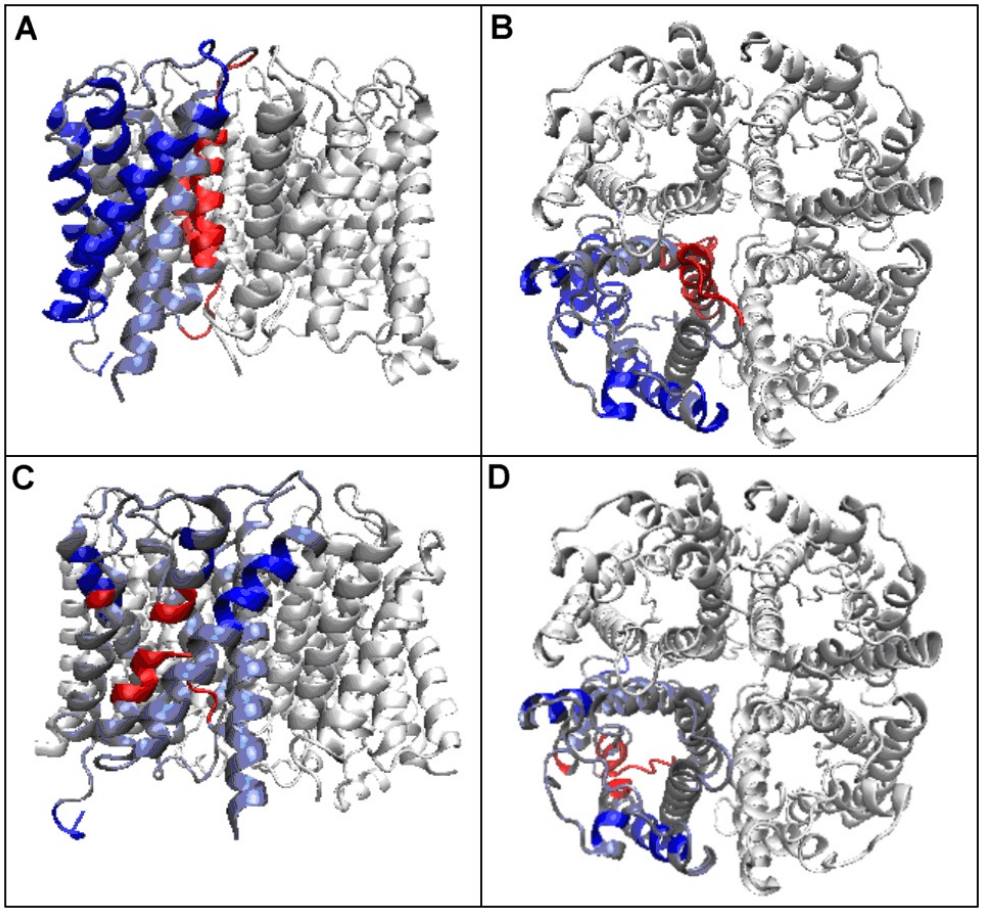

Fig. 4. Two different orientations of the 6QF5 system. (A,B) Reveal the status of the chain as a component of the complex—3D Gaussian function generated for the complete complex. (C,D) Hydrophobicity levels vary within a single chain—3D Gaussian function generated for a single chain treated as an individual structural unit. Sections highlighted in red are local hydrophobicity deficit, and blue are local hydrophobicity excess.

2.3 Programs Used

VMD software was used to visualize the 3D forms of the proteins in question [39,40].

The RD and K values parameters were determined using an open-access server: https://hphob.sano.science/.

3. Results

Table 2 summarizes the results characterizing the human aquaporins of interest. The proteins in question are ordered according to the aquaporin classification. The underlined items are proteins selected for a detailed analysis. The selection was determined by class representation and the degree of structure extension (from a single chain of 1H61 to a complex quaternary structure of 5C5X).

In the detailed analysis, examples with increasing RD values are discussed. These increasing RD values express increasing deviations due to both residues showing a deficit of hydrophobicity in the central part of the molecule/complex, building a channel in the central part, and from the point of view of the exposure of hydrophobic residues on the surface. The exposure of hydrophobic residues for favorable contact with a hydrophobic membrane appears to vary, as shown in [26]. Indeed, the entire surface of some membrane proteins is not covered by hydrophobic residues, thereby allowing protein movement. However, the receptors appear to be stabilized in the membrane, using hydrophobic interactions to engage the whole surface for contact with the membrane. This process probably ensures the receptor is stable, making the addressed communication easier.

An example of the membrane protein aquaporin 1, which is responsible for the passive transport of neutral solutes across lipid bilayer membranes and shows a micelle-like hydrophobicity system (low RD and K values), is presented in Fig. 2. Parameters based on the FOD-M model indicate the presence of a hydrophobic nucleus in the central part of the protein. Such parameters indicate the absence of a channel in the central part of the protein. Therefore, the penetration of water molecules is inhibited, preventing their massive movement. The presence of amino acids showing local hydrophobicity deficit status (the items highlighted in

Table 2. Summary of parameter RD (relative distance) and K (parameter expressing the participation of non-polar compounds in structuralisation) values for the proteins of interest.

PDB ID	Chain	RD	K
1H6I (1)		0.491	0.4
4NEF (2)	A	0.620	0.7
		0.479	0.4
6QF5 (2)	B	0.704	1.1
		0.481	0.4
3DG8 (4)		0.632	0.7
3D9S (5)	A	0.692	1.0
		0.567	0.6
5C5X (5)		0.816	1.1
		0.677	0.9
		0.565	0.6
6QZI (7)	ABCDE	0.605	0.7
6QZJ (7)	B	0.591	0.7
4CSK		0.445	0.4

The numbers presented in parentheses represent the aquaporin classes. The quaternary structure provides the status of the single chain and the set of complexes for 5C5X. The underlined positions represent the proteins discussed in detail in the paper.

red in Fig. 2A) is significantly reduced to just a few items. Exposure to hydrophobicity on the surface also affects a few residues, mainly in the C-terminal section.

T, O, and M profiles visualized the characteristics of aquaporin class 2 using 6QF5 for the corresponding K value, revealing the presence of a channel clearly marked by lower O_i levels against the expected high T_i values. A local excess of O_i hydrophobicity was also identified for low T_i (protein surface area) value levels. These sections are involved in the interaction with the hydrophobic membrane (Fig. 3).

The localization of the relevant sections (local excess, local deficit of hydrophobicity) in the 3D representation highlights the areas involved in transport through the channel (blue residues) and in interaction with the membrane (highlighted in red) (Fig. 4). The summary provided in Figs. 3,4 also reveals a different status depending on the interpretation of the chain as part of a complex and when interpreted as an individual structural unit. This implies differentiated possibilities for transporting water molecules within the complex and a single chain. The interpretation of T, O, and M distributions for a single chain provides insights into the folding of a single chain and its preparation for interaction with other chains and the membrane. Fig. 3B reveals the preparation of the structure rather than function as a component of the complex. The residues showing hydrophobicity exposures in a single chain are not used to complex another chain but rather to interact with the hydrophobic membrane.

A representative of aquaporin class 7, 6QZI, is also discussed here. High RD and K values indicate a hydrophobicity distribution significantly different from the micelle-like system. Similar to the previous example, sections showing a local deficit in hydrophobicity are visible (red sections in Fig. 5A) and local excess hydrophobicity (blue sections in Fig. 4A). These sections indicate fragments of chains responsible for channel structure and interaction with the membrane, respectively (Fig. 5B,C).

The structure represented by 5C5X is an example of the most complex aquaporin system. This set of profiles reveals a repetitive arrangement in all eight chains. As in the previous examples, the sections with a local excess of hydrophobicity are responsible for interacting with the hydrophobic membrane (blue items on the horizontal axis and the residuals involved in channel construction (red items on the axis; Fig. 6)).

The location of the residuals involved in constructing the canal is denoted in red (Fig. 6B,C), and the residues involved in interacting with the membrane are shown in blue (Fig. 6B,C).

An M-function profile close to a line parallel to the X-axis expresses a high value of K = 1.0. This indicates a general structuring reflecting the O arrangement, which is close to the R distribution—all residues show comparable averaged hydrophobicity levels. An interpretation based on the FOD-M model suggests that the folding and construction of the whole system take place in isolation from the polar water environment. It may also be interpreted as an example of structuralisation without a water environment.

The four-chain system (common geometric level) is described by a value of K = 0.8, which is lower than that of the entire complex (eight chains). The localization of sections involved in channel construction and interactions with the membrane are comparable (Fig. 7).

Single chain structuring shows a parameter value of K = 0.5 with slightly different locations of residue positions showing a deficit and a local excess. The sections involved in interacting with chains from the same level show a fairly good match between O_i and T_i levels (Fig. 8A, designated by INTRA). Comparatively, those identified as showing a local excess of hydrophobicity in the N- and C-terminal segments are used for interactions between chains originating from different levels of four-chain systems (Fig. 8A, designated by INTER with 3D presentation given on Fig. 8B,C).

An analysis of the inter-chain interaction reveals an inter-level interaction type of RD = 0.360, which indicates an electrostatic interaction because the fit concerns surface positions. Since the fit is correct, this implies the involvement of surface (polar) residues in the interactions.

The elimination of interactions on the same tier of RD = 0.570 indicates an interface residual status comparable to that of the whole chain. This means that the positions of the residuals involved in this interaction were not singled out for special status. Residues involved in interactions with

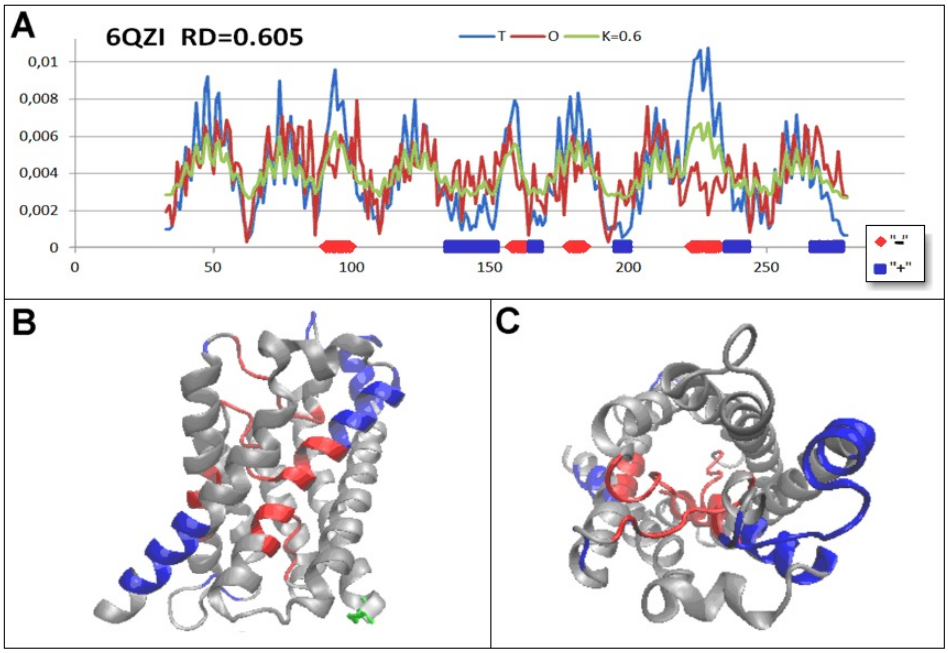

Fig. 5. Characteristics of 6QZI. (A) Summary of T, O, and M profiles for the respective K. Red indicates items showing a deficit in hydrophobicity ("–"); blue indicates a local excess in hydrophobicity ("+"). (B,C) Different 3D orientations of the structure with highlighted sections of local deficit of hydrophobicity (red) and local excess of hydrophobicity (blue). The residuals highlighted in green are the N-terminal position.

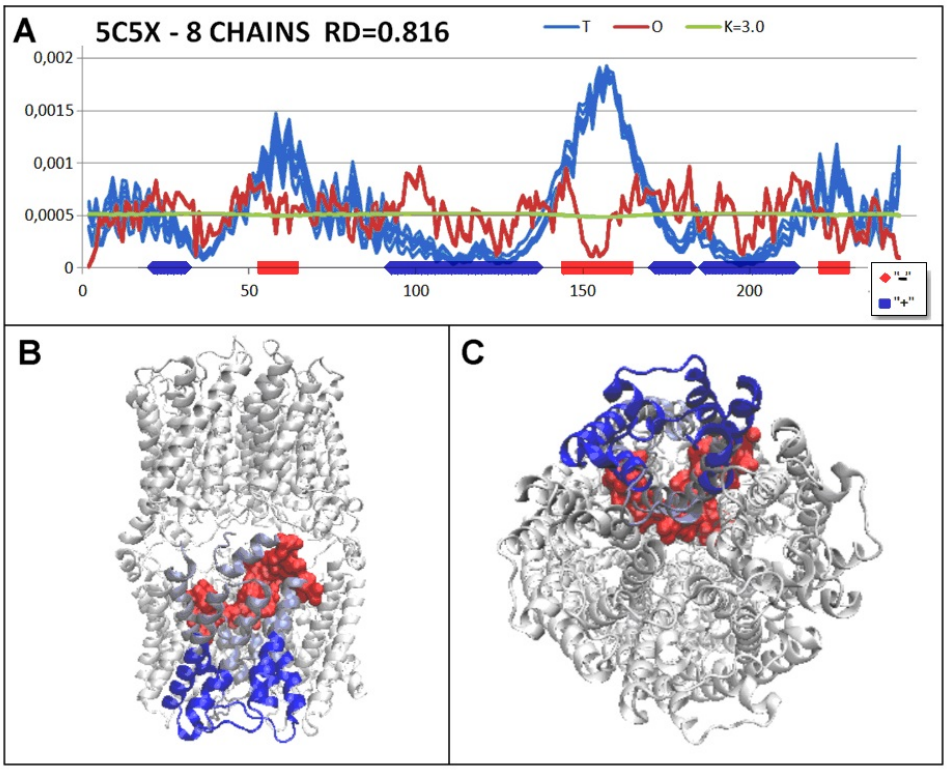

Fig. 6. Characteristics of the 5C5X complex. (A) Summary of T, O, and M profiles for the corresponding K value for all chains (superimposed profiles). Red items: local hydrophobicity deficit ("–"); blue items: local excess hydrophobicity ("+"). (B,C) Two different orientations—3D structure with highlighted sections: red for hydrophobicity deficit and blue for local hydrophobicity excess. Sections are highlighted on the profile set in (A).

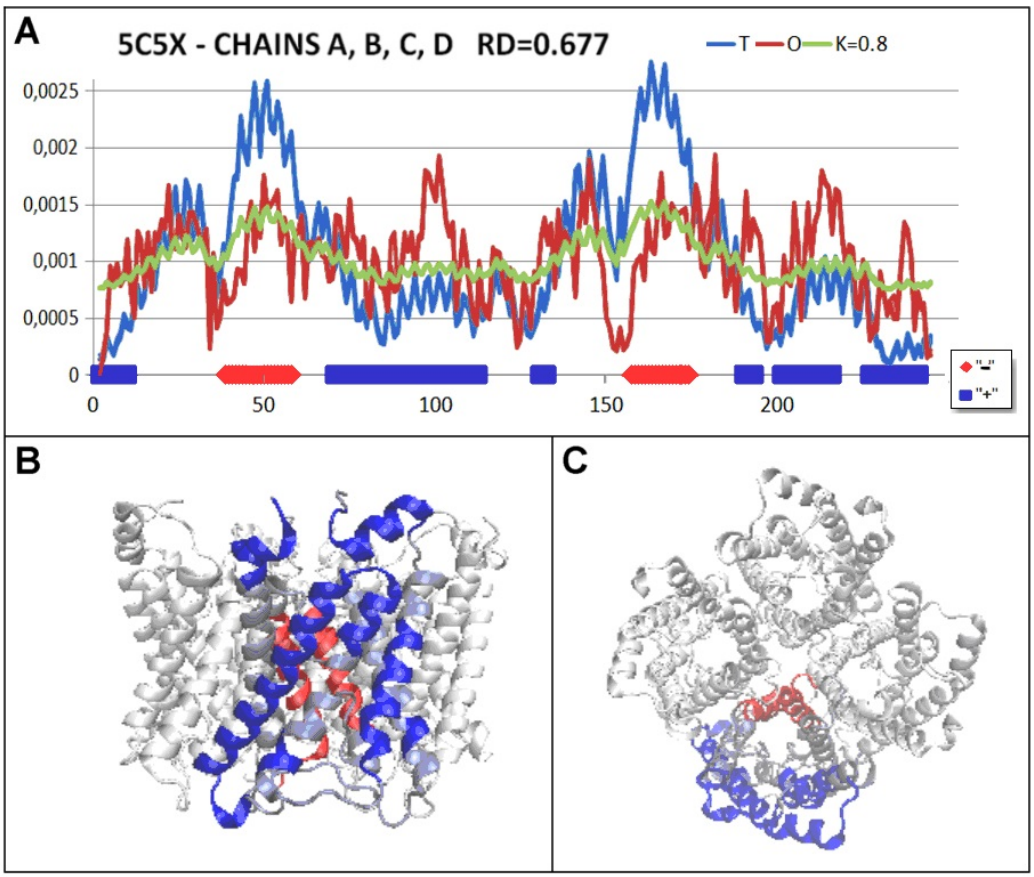

Fig. 7. Characterization of the four-chain part of the 5C5X complex. (A) Summary of T, O, and M profiles for the corresponding K value for all chains (superimposed profiles). Residuals highlighted in red: local hydrophobicity deficit ("–"); residuals highlighted in blue: local hydrophobicity excess ("+"). (B,C) Two different orientations—3D structure with highlighted sections: red for hydrophobicity deficit and blue for local hydrophobicity excess. Sections are highlighted on the profile set in (A).

another chain—if the interaction is through hydrophobic interactions—the status of such an interface should show significantly higher RD values than the status of the whole chain. The status of the part of the chain not involved in interaction with other chains is also comparable (RD = 0.570). This means that structuring has not been subordinated to a special aim of interaction within the quaternary structure.

The main distinguishing feature of this structure is the presence of a channel (hydrophobicity deficit in the central part of the channel.

3.1 Non-Human Aquaporins

To make the comparative analysis possible, the aquaporins representing non-human examples are incorporated into the set of proteins under consideration. The RD and K values for complexes for individual chains are given to characterize the inter-species changes (Table 3, Ref. [8,41–45]).

Table 3. Characteristics of non-human aquaporin examples.

PDB ID	Chain	Source org.	RD	K
8H1D (2) [41]		Bacteria	0.619	0.8
3NE2 (1) [42]		Archaea		
	ABCD		0.663	0.8
	A		0.590	0.5
2W2E (1) [43]		Yeast	0.518	0.3
1Z98 (1) [44]		Plants	0.576	0.5
7W7R (1) [45]		Fish		
	AB		0.740	1.7
	A		0.502	0.4
1J4N (1) [8]		Bovine		
	A		0.414	0.2

The numbers in round parentheses are classes.

3.2 Comparative Analysis of Proteins in Water

The protein folding activity in the water environment and the biological activity in this environment are discussed to complete the comparative analysis. The protein characterized by K = 0.0 is PDB ID: 2LX2, an antifreeze protein [46]. This is an example that follows the rule of micelle con-

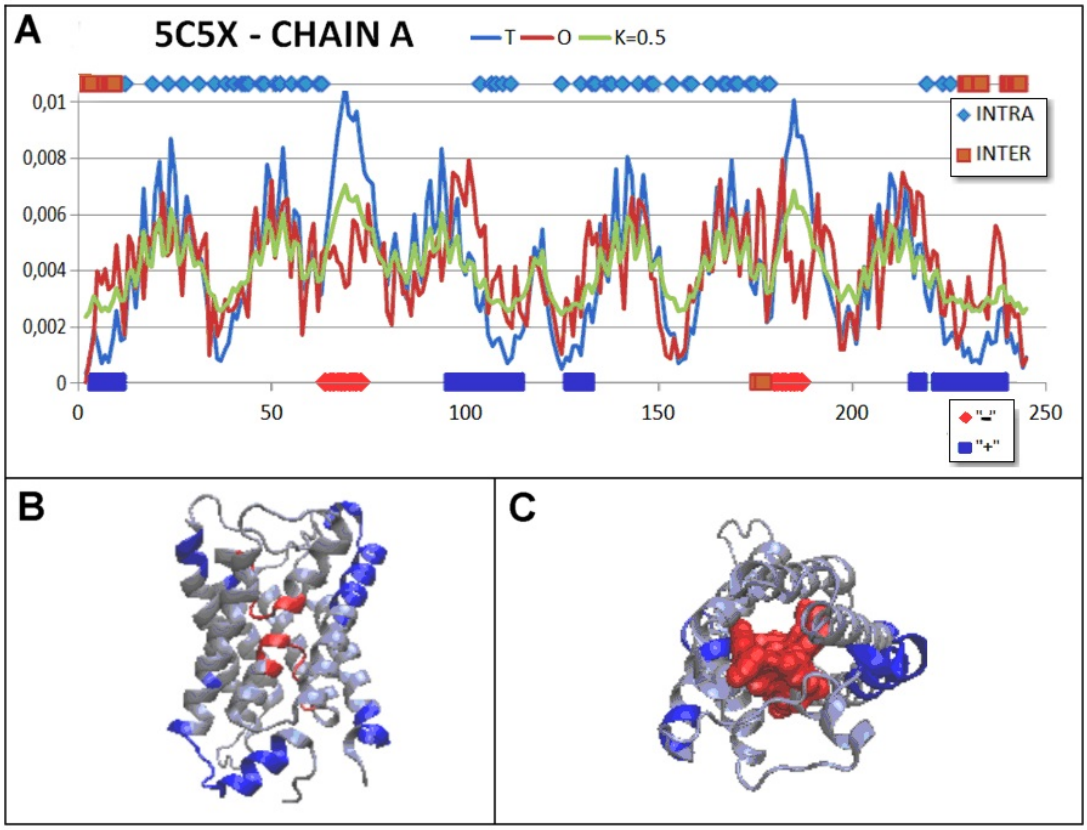

Fig. 8. Characterization of a single chain treated as an individual structural unit (3D Gaussian function spanning a single chain). (A) Summary of T, O, and M profiles for the corresponding K value for a single chain. On the bottom axis, items highlighted in blue have a local excess of hydrophobicity ("+"), while those highlighted in red have a local deficit of hydrophobicity ("–"). The top axis highlights the positions involved in the interaction within one level (INTRA, blue) and between the lower and upper levels (INTER, red). (B,C) Two different orientations—3D structure with highlighted sections: red for hydrophobicity deficit and blue for local hydrophobicity excess. Sections are highlighted on the profile set in (A).

struction. The hydrophobic core is isolated from the water environment by the polar surface, making the protein soluble in water but deprived of any form of specific activity (Fig. 9A). The only expectation for this protein is to order the water molecules according to polar (charged) groups on its surface to resist against the ordering as it appears in ice.

In contrast, the one-chain enzyme oxidoreductase (PDB ID: 1PKF [47]) with K = 0.4 and RD = 0.500 has a local disorder concerning a micelle-like organization, with the rest of the molecule a micelle-like organization. This means solubility is ensured, and the local disorder codes the specificity (Fig. 9B).

Eliminating catalytic residues (D257, T258, T259, C365, and E374) and residues 254-256 as members of the enzymatic cavity (as shown in Fig. 9B, blue dots on the horizontal axis) lowers the RD value for the complete molecule from RD = 0.500 (K = 0.4) to RD = 0.484. This is an example of aim-oriented local discordance coding the specificity of the protein activity.

The next example, one chain (no domains structure) transferase (PDB ID: 3AV4 [48]), represents the status of highly irregular hydrophobicity distribution with respect to a micelle-like distribution. The RD for this protein is equal to 0.734 with K = 1.33. The O distribution differs from the degree of excluding the possibility of identifying residues responsible for discordance dispersed all along the chain (Fig. 9C).

In the context of the alternative examples provided, the analysis of aquaporins seems to be clear as the aim-orientation of hydrophobicity exposition on the surface.

4. Discussion

Exposure of hydrophobic residues on the surface of membrane-anchored proteins is an obvious necessity for stabilizing the cell membrane in a hydrophobic environment. Proteins operating in an aqueous environment greatly adapt the hydrophobicity distribution to the polar water environment. This adaptation forms a micelle-like ordering of the hydrophobicity distribution: a centrally located hydrophobic nucleus with a polar surface, e.g., downhill, fast-folding, ultra-fast-folding, and antifreeze type II proteins mainly belong to this distribution [49].

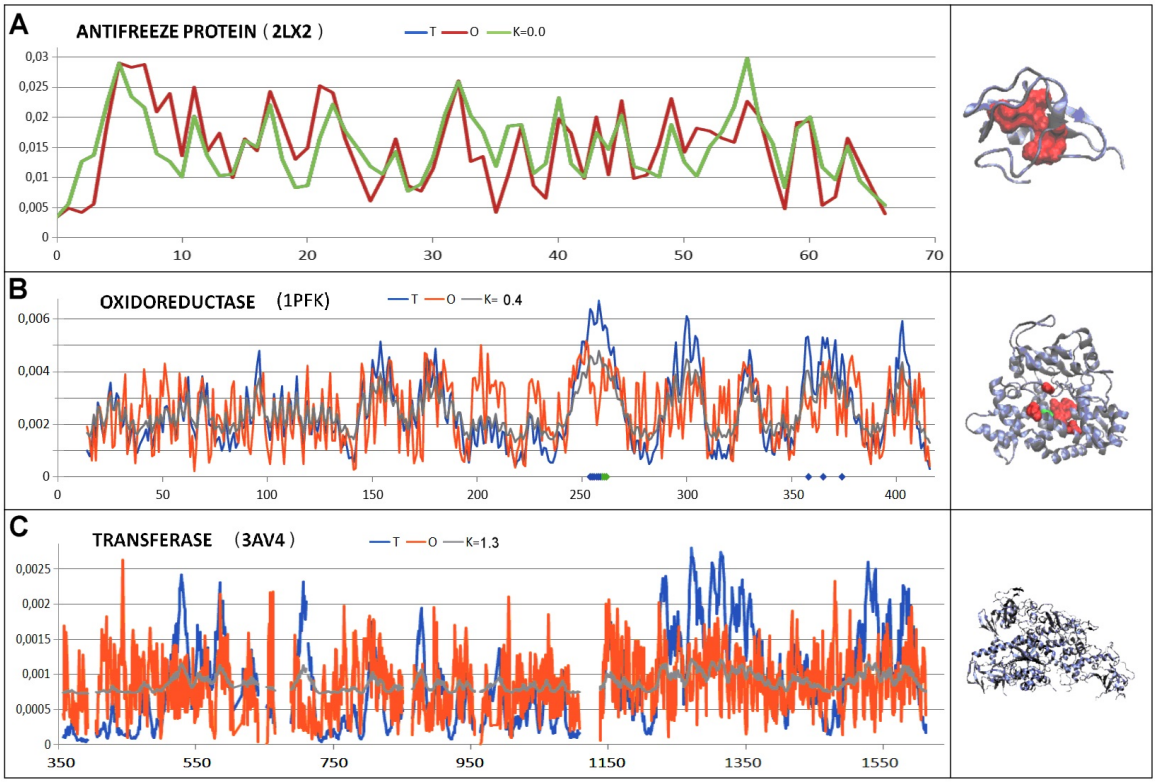

Fig. 9. Examples of proteins acting in a water environment. Profiles T, O, and M (for appropriate K values) are shown with the representative 3D structures. (A) Antifreeze protein is an example of hydrophobicity organization in accordance with the micelle model. K = 0.0 for this protein. (B) Oxidoreductase E.C.2.7.1.11 6-phosphofructokinase from *E. coli*, the hydrophobicity organization in this protein is represented by K = 0.4. Catalytic residues are red in the 3D presentation (distinguished on the x-axis: catalytic residues). The residues distinguished in green on the x-axis and green on the 3D presentation represent the cavity. (C) Transferase—E.C.2.1.1.37—DNA (cytosine-5-)-methyltransferase: an example of a protein with hydrophobicity distribution deprived of a hydrophobic core; no micelle-like organization identified in this protein. The K value is very high, K = 1.3.

The distribution of hydrophobicity appears to reflect specific activity by generating cavities prepared for substrate interaction in enzymes. A cavity is recognized as a local hydrophobicity deficit [49]. Meanwhile, environmental conditions are essential in differentiating the folding process through specific orientations. This phenomenon is critical for protein structure prediction methods in the critical assessment of structure prediction (CASP) project [50].

The presence of a membrane protein with a micelle-like distribution (1H6I) suggests the absence of a channel or possibly a "closed" structure. Such an example has already been observed with the outer membrane beta-barrel transmembrane protein (PDB ID: 2LHF), where antibiotic resistance has been experimentally identified [51]. The ordered condition of hydrophobicity in a micelle-like form with a centrally located hydrophobic nucleus is interpreted as resistant to the transportation process of any molecule.

The proteins discussed here—aquaporins—show the expected structuring required for their function. Individual chains show varying degrees of order at the RD scale. The central aspect—the channel part—shows in all the proteins in question the clear deficit of hydrophobicity with an exposure of hydrophobicity on sections located on the surface, similar to the examples discussed [26]. The mode of anchorage is varied—restricted to selected relevant fragments of the protein chain. The expected complete coverage of the protein's contact surface with hydrophobic residues on the membrane is not found, except in examples of extended receptors, where stabilization of localization appears to be important for the biological function performed by the receptors. The partial involvement of only selected chain fragments in interacting with the hydrophobic membrane may allow limited mobility and specific structural variability under membrane conditions. The analysis presented here is another example of an aim-oriented folding process in which the role of the environment proves to be critical for stabilizing a structure that guarantees biological function.

The FOD-M model also reveals the ubiquity and fundamental role of the aquatic environment (Eqn. 7). The 3D Gaussian function is always present, which means that the water environment is always involved. Thus, modifying the 3D Gaussian function, expressed as the value of the parameter K, can reveal the variation in protein folding conditions.

5. Conclusions

The conclusion of the presented material is to demonstrate the necessary presence of external conditions in the folding process. The section on protein structure prediction seems to be solved by AlphaFold [52]. However, the question, "Why do the proteins fold the way they do?" remains unclear. This study has shown that the energy status, according to assumptions, can represent the minimal internal energy appropriate for external conditions. Thus, the optimization procedure in the protein folding process simulation depends on the internal force field (non-bonding interaction inside the protein body) and external force field (influence of environment).

The analysis can be applied in the process of *de novo* protein design. The applied model FOD-M can be used for any hydrophobic scale, as shown in [53].

Availability of Data and Materials

All data can be reconstructed by the Reader using the open access server given in Programs used section.

Author Contributions

Conceptualization: IR and LK. Data collection and analysis: KS, DD, GS. Manuscript preparation: IR, GS and KS. All authors contributed to editorial changes in the manuscript. All authors read and approved the final manuscript. All authors have participated sufficiently in the work and agreed to be accountable for all aspects of the work.

Ethics Approval and Consent to Participate

Not applicable.

Acknowledgment

Many thanks to Anna Smietanska and Zdzislaw Wisniowski for technical help.

Funding

This research was funded by Jagiellonian University Medical College, grant number N41/DBS/000722. This research was partially supported by the European Union's Horizon 2020 Program under grant no. 857533 and the Sano project carried out within the International Research Agendas Program of the Foundation for Polish Science and was co-financed by the European Union under the European Regional Development Fund. We also gratefully acknowledge Polish high-performance computing infrastructure PLGrid (HPC Center: ACK Cyfronet AGH) for providing computer facilities and support within computational grant no. PLG/2024/01739. Funding is related to the manuscript topic.

Conflict of Interest

All authors declare no conflicts of interest. Despite Dawid Dułak is from ABB Business Services Sp. z o.o, the judgments in data interpretation and writing were not influenced by this relationship.

References

[1] Agre P. The aquaporin water channels. Proceedings of the American Thoracic Society. 2006; 3: 5–13. https://doi.org/10.1513/pats.200510-109JH.

[2] Brown D. The Discovery of Water Channels (Aquaporins). Annals of Nutrition & Metabolism. 2017; 70: 37–42. https://doi.org/10.1159/000463061.

[3] Sehy JV, Banks AA, Ackerman JJH, Neil JJ. Importance of intracellular water apparent diffusion to the measurement of membrane permeability. Biophysical Journal. 2002; 83: 2856–2863. https://doi.org/10.1016/S0006-3495(02)75294-6.

[4] Verkman AS, Mitra AK. Structure and function of aquaporin water channels. American Journal of Physiology. Renal Physiology. 2000; 278: F13–F28. https://doi.org/10.1152/ajprenal.2000.278.1.F13.

[5] Hedfalk K, Törnroth-Horsefield S, Nyblom M, Johanson U, Kjellbom P, Neutze R. Aquaporin gating. Current Opinion in Structural Biology. 2006; 16: 447–456. https://doi.org/10.1016/j.sbi.2006.06.009.

[6] Huang B, Wang H, Yang B. Non-Aquaporin Water Channels. Advances in Experimental Medicine and Biology. 2023; 1398: 331–342. https://doi.org/10.1007/978-981-19-7415-1_23.

[7] de Groot BL, Grubmüller H. Water permeation across biological membranes: mechanism and dynamics of aquaporin-1 and GlpF. Science. 2001; 294: 2353–2357. https://doi.org/10.1126/science.1066115.

[8] Sui H, Han BG, Lee JK, Walian P, Jap BK. Structural basis of water-specific transport through the AQP1 water channel. Nature. 2001; 414: 872–878. https://doi.org/10.1038/414872a.

[9] Bollag WB, Aitkens L, White J, Hyndman KA. Aquaporin-3 in the epidermis: more than skin deep. American Journal of Physiology. Cell Physiology. 2020; 318: C1144–C1153. https://doi.org/10.1152/ajpcell.00075.2020.

[10] Papadopoulos MC, Verkman AS. Aquaporin water channels in the nervous system. Nature Reviews. Neuroscience. 2013; 14: 265–277. https://doi.org/10.1038/nrn3468.

[11] D'Agostino C, Parisis D, Chivasso C, Hajiabbas M, Soyfoo MS, Delporte C. Aquaporin-5 Dynamic Regulation. International Journal of Molecular Sciences. 2023; 24: 1889. https://doi.org/10.3390/ijms24031889.

[12] Login FH, Nejsum LN. Aquaporin water channels: roles beyond renal water handling. Nature Reviews. Nephrology. 2023; 19: 604–618. https://doi.org/10.1038/s41581-023-00734-9.

[13] Kitchen P, Salman MM, Halsey AM, Clarke-Bland C, MacDonald JA, Ishida H, *et al*. Targeting Aquaporin-4 Subcellular Localization to Treat Central Nervous System Edema. Cell. 2020; 181: 784–799.e19. https://doi.org/10.1016/j.cell.2020.03.037.

[14] Sylvain NJ, Salman MM, Pushie MJ, Hou H, Meher V, Herlo R, *et al*. The effects of trifluoperazine on brain edema, aquaporin-4 expression and metabolic markers during the acute phase of stroke using photothrombotic mouse model. Biochimica et Biophysica Acta. Biomembranes. 2021; 1863: 183573. https://doi.org/10.1016/j.bbamem.2021.183573.

[15] Abir-Awan M, Kitchen P, Salman MM, Conner MT, Conner AC, Bill RM. Inhibitors of Mammalian Aquaporin Water Channels. International Journal of Molecular Sciences. 2019; 20: 1589. https://doi.org/10.3390/ijms20071589.

[16] Wevers NR, Kasi DG, Gray T, Wilschut KJ, Smith B, van Vught

R, *et al*. A perfused human blood-brain barrier on-a-chip for high-throughput assessment of barrier function and antibody transport. Fluids and Barriers of the CNS. 2018; 15: 23. https://doi.org/10.1186/s12987-018-0108-3.

[17] Salman MM, Kitchen P, Woodroofe MN, Brown JE, Bill RM, Conner AC, *et al*. Hypothermia increases aquaporin 4 (AQP4) plasma membrane abundance in human primary cortical astrocytes via a calcium/transient receptor potential vanilloid 4 (TRPV4)- and calmodulin-mediated mechanism. The European Journal of Neuroscience. 2017; 46: 2542–2547. https://doi.org/10.1111/ejn.13723.

[18] Ciappelloni S, Bouchet D, Dubourdieu N, Boué-Grabot E, Kellermayer B, Manso C, *et al*. Aquaporin-4 Surface Trafficking Regulates Astrocytic Process Motility and Synaptic Activity in Health and Autoimmune Disease. Cell Reports. 2019; 27: 3860–3872.e4. https://doi.org/10.1016/j.celrep.2019.05.097.

[19] Salman MM, Kitchen P, Halsey A, Wang MX, Törnroth-Horsefield S, Conner AC, *et al*. Emerging roles for dynamic aquaporin-4 subcellular relocalization in CNS water homeostasis. Brain. 2022; 145: 64–75. https://doi.org/10.1093/brain/awab311.

[20] Aldewachi H, Al-Zidan RN, Conner MT, Salman MM. High-Throughput Screening Platforms in the Discovery of Novel Drugs for Neurodegenerative Diseases. Bioengineering. 2021; 8: 30. https://doi.org/10.3390/bioengineering8020030.

[21] Roterman I, Stapor K, Fabian P, Konieczny L, Banach M. Model of Environmental Membrane Field for Transmembrane Proteins. International Journal of Molecular Sciences. 2021; 22: 3619. https://doi.org/10.3390/ijms22073619.

[22] Roterman I, Stapor K, Gądek K, Gubała T, Nowakowski P, Fabian P, *et al*. Dependence of Protein Structure on Environment: FOD Model Applied to Membrane Proteins. Membranes. 2021; 12: 50. https://doi.org/10.3390/membranes12010050.

[23] Roterman I, Stapor K, Fabian P, Konieczny L. The Functional Significance of Hydrophobic Residue Distribution in Bacterial Beta-Barrel Transmembrane Proteins. Membranes. 2021; 11: 580. https://doi.org/10.3390/membranes11080580.

[24] Roterman I, Stapor K, Konieczny L. The Contribution of Hydrophobic Interactions to Conformational Changes of Inward/Outward Transmembrane Transport Proteins. Membranes. 2022; 12: 1212. https://doi.org/10.3390/membranes12121212.

[25] Roterman I, Stapor K, Fabian P, Konieczny L. Connexins and Pannexins-Similarities and Differences According to the FOD-M Model. Biomedicines. 2022; 10: 1504. https://doi.org/10.3390/biomedicines10071504.

[26] Roterman I, Stapor K, Konieczny L. Transmembrane proteins-Different anchoring systems. Proteins. 2024; 92: 593–609. https://doi.org/10.1002/prot.26646.

[27] Berman HM, Westbrook J, Feng Z, Gilliland G, Bhat TN, Weissig H, *et al*. The Protein Data Bank. Nucleic Acids Research. 2000; 28: 235–242. https://doi.org/10.1093/nar/28.1.235.

[28] de Groot BL, Engel A, Grubmüller H. A refined structure of human aquaporin-1. FEBS Letters. 2001; 504: 206–211. https://doi.org/10.1016/s0014-5793(01)02743-0.

[29] Frick A, Eriksson UK, de Mattia F, Oberg F, Hedfalk K, Neutze R, *et al*. X-ray structure of human aquaporin 2 and its implications for nephrogenic diabetes insipidus and trafficking. Proceedings of the National Academy of Sciences of the United States of America. 2014; 111: 6305–6310. https://doi.org/10.1073/pnas.1321406111.

[30] Lieske J, Cerv M, Kreida S, Komadina D, Fischer J, Barthelmess M, *et al*. On-chip crystallization for serial crystallography experiments and on-chip ligand-binding studies. IUCrJ. 2019; 6: 714–728. https://doi.org/10.1107/S2052252519007395.

[31] Dasgupta T, Chitnumsub P, Kamchonwongpaisan S, Maneeruttanarungroj C, Nichols SE, Lyons TM, *et al*. Exploiting structural analysis, in silico screening, and serendipity to identify novel inhibitors of drug-resistant falciparum malaria. ACS Chemical Biology. 2009; 4: 29–40. https://doi.org/10.1021/cb8002804.

[32] Horsefield R, Nordén K, Fellert M, Backmark A, Törnroth-Horsefield S, Terwisscha van Scheltinga AC, *et al*. High-resolution x-ray structure of human aquaporin 5. Proceedings of the National Academy of Sciences of the United States of America. 2008; 105: 13327–13332. https://doi.org/10.1073/pnas.0801466105.

[33] Kitchen P, Öberg F, Sjöhamn J, Hedfalk K, Bill RM, Conner AC, *et al*. Plasma Membrane Abundance of Human Aquaporin 5 Is Dynamically Regulated by Multiple Pathways. PLoS ONE. 2015; 10: e0143027. https://doi.org/10.1371/journal.pone.0143027.

[34] de Maré SW, Venskutonytė R, Eltschkner S, de Groot BL, Lindkvist-Petersson K. Structural Basis for Glycerol Efflux and Selectivity of Human Aquaporin 7. Structure. 2020; 28: 215–222.e3. https://doi.org/10.1016/j.str.2019.11.011.

[35] Ruiz Carrillo D, To Yiu Ying J, Darwis D, Soon CH, Cornvik T, Torres J, *et al*. Crystallization and preliminary crystallographic analysis of human aquaporin 1 at a resolution of 3.28 Å. Acta Crystallographica. Section F, Structural Biology Communications. 2014; 70: 1657–1663. https://doi.org/10.1107/S2053230X14024558.

[36] Roterman I, Konieczny L. Protein Is an Intelligent Micelle. Entropy. 2023; 25: 850. https://doi.org/10.3390/e25060850.

[37] Levitt M. A simplified representation of protein conformations for rapid simulation of protein folding. Journal of Molecular Biology. 1976; 104: 59–107. https://doi.org/10.1016/0022-2836(76)90004-8.

[38] Kullback S, Leibler RA. On information and sufficiency. The Annals of Mathematical Statistics. 1951; 22: 79–86. https://doi.org/10.1214/aoms/1177729694.

[39] Visual Molecular Dynamics. Available at: https://www.ks.uiuc.edu/Research/vmd/ (Accessed: 26 January 2024).

[40] Humphrey W, Dalke A, Schulten K. VMD: visual molecular dynamics. Journal of Molecular Graphics. 1996; 14: 33–38, 27–28. https://doi.org/10.1016/0263-7855(96)00018-5.

[41] Xie H, Zhao Y, Zhao W, Chen Y, Liu M, Yang J. Solid-state NMR structure determination of a membrane protein in *E. coli* cellular inner membrane. Science Advances. 2023; 9: eadh4168. https://doi.org/10.1126/sciadv.adh4168.

[42] Lee JK, Finer-Moore JS, Stroud RM. Available at: https://www.rcsb.org/structure/3ne2 (Accessed: 26 January 2024).

[43] Fischer G, Kosinska-Eriksson U, Aponte-Santamaría C, Palmgren M, Geijer C, Hedfalk K, *et al*. Crystal structure of a yeast aquaporin at 1.15 angstrom reveals a novel gating mechanism. PLoS Biology. 2009; 7: e1000130. https://doi.org/10.1371/journal.pbio.1000130.

[44] Törnroth-Horsefield S, Wang Y, Hedfalk K, Johanson U, Karlsson M, Tajkhorshid E, *et al*. Structural mechanism of plant aquaporin gating. Nature. 2006; 439: 688–694. https://doi.org/10.1038/nature04316.

[45] Zeng J, Schmitz F, Isaksson S, Glas J, Arbab O, Andersson M, *et al*. High-resolution structure of a fish aquaporin reveals a novel extracellular fold. Life Science Alliance. 2022; 5: e202201491. https://doi.org/10.26508/lsa.202201491.

[46] Kumeta H, Ogura K, Nishimiya Y, Miura A, Inagaki F, Tsuda S. NMR structure note: a defective isoform and its activity-improved variant of a type III antifreeze protein from Zoarces elongates Kner. Journal of Biomolecular NMR. 2013; 55: 225–230. https://doi.org/10.1007/s10858-012-9703-9.

[47] Shirakihara Y, Evans PR. Crystal structure of the complex of phosphofructokinase from Escherichia coli with its reaction products. Journal of Molecular Biology. 1988; 204: 973–994.

https://doi.org/10.1016/0022-2836(88)90056-3.
[48] Takeshita K, Suetake I, Yamashita E, Suga M, Narita H, Nakagawa A, *et al*. Structural insight into maintenance methylation by mouse DNA methyltransferase 1 (Dnmt1). Proceedings of the National Academy of Sciences of the United States of America. 2011; 108: 9055–9059. https://doi.org/10.1073/pnas.1019629108.
[49] Banach M, Stapor K, Konieczny L, Fabian P, Roterman I. Downhill, Ultrafast and Fast Folding Proteins Revised. International Journal of Molecular Sciences. 2020; 21: 7632. https://doi.org/10.3390/ijms21207632.
[50] Roterman I, Stapor K, Konieczny L. Role of environmental specificity in CASP results. BMC Bioinformatics. 2023; 24: 425. https://doi.org/10.1186/s12859-023-05559-8.
[51] Edrington TC, Kintz E, Goldberg JB, Tamm LK. Structural basis for the interaction of lipopolysaccharide with outer membrane protein H (OprH) from Pseudomonas aeruginosa. The Journal of Biological Chemistry. 2011; 286: 39211–39223. https://doi.org/10.1074/jbc.M111.280933.
[52] Abramson J, Adler J, Dunger J, Evans R, Green T, Pritzel A, *et al*. Accurate structure prediction of biomolecular interactions with AlphaFold 3. Nature. 2024; 630: 493–500. https://doi.org/10.1038/s41586-024-07487-w.
[53] Kalinowska B, Banach M, Konieczny L, Roterman I. Application of Divergence Entropy to Characterize the Structure of the Hydrophobic Core in DNA Interacting Proteins. Entropy. 2015; 17: 1477–1507. https://doi.org/10.3390/e17031477.